CPOP: An open source C++ cell POPulation modeler for radiation biology applications

L. Maigne, A. Delsol, G. Fois, E. Debiton, F. Degoul, H. Payno

CPOP : an open source C++ Cell POPulation modeler for radiation biology applications.

L. Maigne[1], A. Delsol[1], G. Fois[1], E. Debiton[2,3], F. Degoul[2,3], H. Payno[1]

[1]Université Clermont Auvergne, CNRS/IN2P3, LPC, 63000 Clermont-Ferrand, France.

[2]INSERM, 1240, 58 Rue Montalembert, 63 005 Clermont-Ferrand cedex, France.

[3]Université Clermont Auvergne, Imagerie Moléculaire et Stratégies Théranostiques, BP 10448, 63000 Clermont-Ferrand France.

Corresponding author: Lydia.Maigne@clermont.in2p3.fr

Abstract

Purpose

Multicellular tumor spheroids are realistic in-vitro systems used in radiation biology research to study the effect of anticancer drugs or to evaluate the resistance of cancer cells under specific conditions. When combining the modeling of spheroids together with the simulation of radiation using Monte Carlo methods, one could estimate cell and DNA damage to be compared with experimental data. We developed a Cell Population (CPOP) modeler combined to Geant4 simulations in order to tackle how energy depositions are allocated to cells, especially when enhancing radiation outcomes using high-Z nanoparticles. CPOP manages to model large three-dimensional cell populations with independent deformable cells described with their nucleus, cytoplasm and membranes together with force law systems to manage cell-cell interactions.

Methods

CPOP is an opensource platform written in C++. It is divided into two main libraries: a “Modeler” library, for cell geometry modeling using meshes, and a Multi Agent System (MAS) library, simulating all agent (cell) interactions among the population. CPOP is fully interfaced with the Geant4 Monte Carlo toolkit and is able to directly launch Geant4 simulations after compilation.

We modeled a full and realistic 3D cell population from SK-MEL28 melanoma cell population cultured experimentally. The spheroid diameter of 550±40 µm corresponds to a population of approximately 1000 cells

having a diameter of 17.2±2.5 µm and a nucleus diameter of 11.2±2.0 µm. We decided to reproduce cell irradiations performed with a X-RAD 320 Biological Irradiator (Precision XRay Inc., North Branford, CT).

Results

We simulated the energy spectrum of secondary particles generated in the vicinity of the spheroid and plotted the different energy spectra recovered internally to the spheroid. We evaluated also the impact of AGuIX (Gadolinium) nanoparticles modeled into the spheroid with their corresponding secondary energy spectra.

Conclusions

We succeeded into modeling cell populations and combined them with Geant4 simulations. The next step will be to integrate DNA geometrical models into cell nuclei and to use the Geant4-DNA physics and radiolysis modeling capabilities in order to evaluate early strand breaks induced on DNA.

Key words: cell population, Monte Carlo, Geant4, GATE, radiation biology, nanoparticles

1. Introduction

In-silico modeling of 2D (monolayer) and 3D (spheroid) cell populations is often necessary to better characterize their experimental behavior while they are subjected to different environmental constraints such as: cell interactions, hypoxia [1], nutrient limitations or ionizing radiations. Multicellular tumor spheroids are realistic in-vitro systems used in radiation biology research to study the effect of anticancer drugs or to evaluate the resistance of cancer cells especially with nanomedicine approaches [2]. When combining the modeling of spheroids together with the simulation of radiation therapy treatments (using Monte Carlo methods for example), one could estimate cell and DNA damage to be compared with experimental endpoints. This is particularly relevant when studying the impact of radio-sensitizers such as gadolinium-based nanoparticles (GBNs) penetrating multicellular tumor spheroids in the objective to initiate interesting therapeutic outcomes for notably radio-resistant tumors. Different authors studied the impact of nanoparticles on radiation therapy outcomes with the help of Monte Carlo simulations but only in a liquid water medium. Some authors, like Taupin et al. [3], computed a macroscopic physical dose enhancement factor (DEF) produced by GBNs under radiation (monoenergetic photon beams of energy between 2 keV and 10 MeV) by modeling different amount of GBNs in a large liquid water medium with the PENELOPE code [4]. Jones et al. [5] and Chow et al. [6] studied the microscopic dose enhancement due to gold nanoparticles under low energy photon sources by computing radial dose distribution around electron dose kernels with the NOREC code [7]. Li et al. [8,9] studied the same topic by intercomparing different codes. Sakata et al. [10] and Poignant et al. [11] proposed electron track structure simulations for gold nanoparticles using Geant4-DNA and MDM codes. Similar Monte Carlo studies have been published in proton therapy [12–17] using different codes. McKinnon et al. [16,17] computed energy deposition on a nanoscale around a single nanoparticle of 100 nm diameter using the Geant4-DNA extension [18,19].

In this context, accurate identification and understanding of cellular and molecular damage requires efficient and cross platform libraries able to answer biologists and radiation physicists needs.

In this paper, we present the CPOP object-oriented (C++) open-source cell population modeler, under GNU Lesser General Public Licence version 3, implemented in the objective to provide realistic 2D and 3D cell

populations mimicking in vitro configurations. The C++ open-source platform development was guided by the following list of requirements:

- Ability to model 2D and 3D cell populations containing up to a million of cells,
- Ability to model 2D and 3D independent deformable cells with their organelles such as nucleus, cytoplasm and membrane,
- Ability to define force law systems for cell-cell interactions,
- Compatibility with Monte Carlo simulations to study radiation effects on cell populations,
- Ability to provide an ergonomic API for users to fix their own cell population parameters such as number of cells, size of cells, force laws…

Different methods [20–26] have been proposed to model cell population. Barberet et al. [27] implemented a method based on high resolution confocal imaging and ion beam analysis in order to obtain realistic cell nucleus geometry; however this method requires a fully dedicated image reconstruction process that is most of the time not easily accessible to users. Other solutions propose to build cell population by estimating cell parameters from measurable data or from theoretical values. Existing free and open source software such as Chaste [28] or CompuCell3D [29] are able to propose cell population models based on these parameters to initiate cell clustering as well as growth, division, death, intracellular adhesion, volume and surface area constraints and include dedicated cellular automata for categorizing cells. Nevertheless, those toolkits do not offer the possibility to obtain deformable cell shapes with dynamic radii that would fit accurately experimental outcomes.

The CPOP platform proposes dedicated meshes to distort each cell using a dynamic radius to obtain a high-level conformation of cell membranes with their neighbours. Furthermore, CPOP is able to deal with large cell populations (multicellular spheroids) reaching over one million of cells. In order to implement those features, we used the well-known CGAL library [30]. It has to be noticed that, contrary to Chaste and CompuCell3D software, CPOP does not propose to model cell population growth but represents cell populations in their final state when the cell population has reached a size and a number of cells corresponding to what is observed with microscopy. Spatial positions of each cell and organelle in the cell population are accessible in CPOP.

The CPOP platform has been interfaced to the Geant4 toolkit [31–34] in order to tackle how energy depositions are allocated to cells, especially when enhancing radiation outcomes using gold or gadolinium nanoparticles. Some authors already assessed such outcomes when simulating ceramic oxide nanoparticles under MeV proton irradiation or kilovoltage photon field [16,17,35]. For that purpose, they used simplified cell geometry to mimic experimental observations on 2D cell populations (gliosarcoma cells).

This work proposes a new platform, the CPOP platform, to investigate radiation damage on realistic cell populations. Therefore, in this article, we start by presenting the experimental background study to characterize 3D cell models that enabled the set-up of the list of requirements to develop the platform. After describing the capabilities in building realistic geometry of cell populations, with the description of the multicellular population conformation, the meshing algorithms proposed, the management of inputs/outputs and the extended functionalities; we show how the platform can assess the different energy spectra in the characteristic layers of 3D cell populations. Finally, we evaluate the impact of GBN concentration on energy enhancement in the cell population under orthovoltage beam. All energy spectra used as inputs to the CPOP platform have been simulated using the GATE Monte Carlo platform [36–38]. GATE is a C++ and open-source platform making a wide range of GEANT4 functionality available through a user-friendly interface. The platform has come into widespread use in the field of imaging (PET, SPECT, CT) and radiation therapy. In a near future, the objective is to merge the CPOP features to the GATE platform.

2. Material and Methods

2.1 Characterization of 3D cell models

In the objective to develop the best-suited platform for the modeling of 3D cell populations, an experimental set-up has been validated to produce 3D cell models. Human SK-MEL 28 melanoma cells (usually radiation resistant cancer cells) are maintained in MEM Glutamax™ supplemented with 10% FCS and 4µg/mL gentamicin and are grown at 37°C in humidified incubator containing 5% CO2. 3D cell populations are obtained by adding 0.5% methylcellulose to the suitable culture medium. 3D cells are then seeded in 100µl of medium in V-shaped

96-well plates. Spheroid diameters are measured between day 1 and day 4 by conventional reverse-phased microscopy (Eclipse TS100, Nikon Instruments, Tokyo, Japan); during this period, diameter lengths are varying from 400±50 µm to 550±40 µm. At day 4, the spheroid diameter of 550±40 µm corresponds to approximately 1000 cells having a diameter of 17.2±2.5 µm and a nucleus diameter of 11.2±2.0 µm. In Figure 1 (a) is presented a spheroid of melanoma cancer cells, SK-MEL 28 type of 550±40 µm in diameter obtained by conventional microscopy. Figure 1 (b) presents the same type of cancer cells imaged with a fluorescent confocal microscopy using a lipophilic dye CellMask™ Orange (excitation 554 nm/emission 567 nm) (Invitrogen) staining membranes, and the classic DAPI staining DNA (Sigma, Les Arbresles, France) to visualize nuclear compartment on a Leica SPE microscope (Leica Biosystems, Nussloch GmbH).

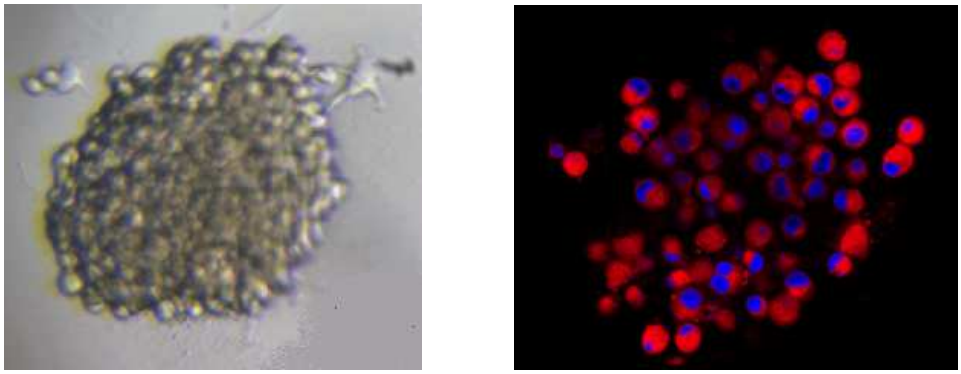

(a) (b)

Figure 1. (a) Reverse-phased microscopy imaging of a spheroid (SK-MEL 28 type) of 550±40 µm in diameter (b) Fluorescent confocal microscopy of a spheroid (SK-MEL 28 type)

2.2 CPOP architecture

CPOP is an opensource C++ platform dedicated to the modeling of radiobiological experiments, typically large spherical 3D cell populations undergoing ionizing radiation. As strong requirement, this tool should be fully compatible with Geant4 simulations and in a later version with GATE simulations.

The CPOP platform is divided into two main libraries. The first library, named “Modeler”, corresponds to the modeling of cell populations. It embeds two family classes, “Geometry” and “Models”, related to the geometry and to models chosen to create each cell.

The second library is related to the implementation of the Multi Agent System (MAS) embedding the "MASPlatform" family class simulating all agents involved with the "Agent" family class. Each agent corresponds to a cell. This library is managing all the processes concerning the cell population simulation. The simplified class diagram of the CPOP platform is presented in Figure 2.

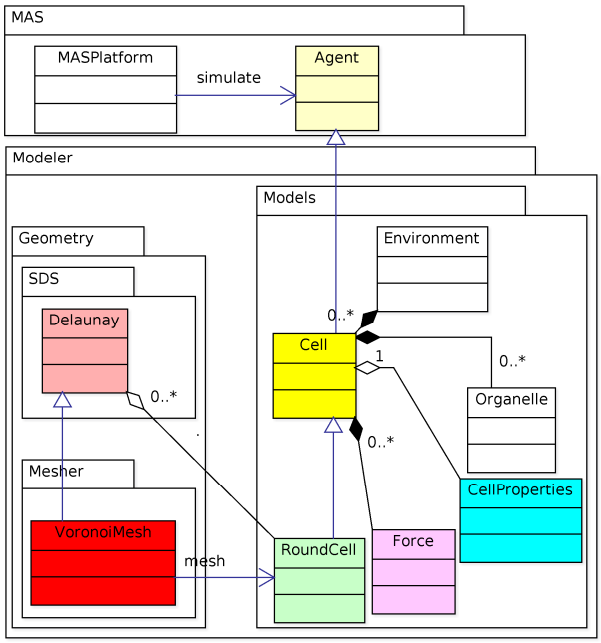

Figure 2. Simplified class diagram of the CPOP platform

2.2.1 Compilation

CPOP version 2.0 is compatible with Linux OS and gcc version 4.8 and higher. Before compiling the CPOP platform, it is necessary to install some open-source programs and libraries. First, it is mandatory to install Qt (http://www.qt.io/), version 4.6 or later, in order to empower Man-Machine Interface (MMI) utilities and engines. Then, it is required to install CGAL libraries version 4.5 (http://www.cgal.org/) in order to benefit from Delaunay and Voronoi facilities to build respectively triangulation and meshes for cell populations. This installation is requiring Boost (http://www.boost.org/), MPFR (http://www.mpfr.org/) and Xerces C++ libraries (http://xerces.apache.org/, version 2.0 or later); the latter enables XML parsing when GDML exportation of cell population geometry is performed. In order to display any geometry built with CPOP, it is necessary to install QGLViewer, version 2.0 or later (http://libqglviewer.com/). Then, in order to interface

CPOP with Geant4 simulations (http://geant4.org), users would have to install the toolkit on their computer; the installation of Geant4 requires an external installation of CLHEP (A Class Library for High Energy Physics, http:// http://proj-clhep.web.cern.ch/, version 2.1.4.1). Therefore, users may pay attention to fix the GEANT4_USE_SYSTEM_CLHEP option to ON during the Geant4 compilation and to fix the WITH_EXTERNAL_CLHEP option to ON during the CPOP compilation. Further, the ROOT Data analysis framework (https://root.cern.ch/, version 5.34 or later) has to be installed to enable data outputs at the end of particle tracking simulations inside cell populations. The compilation of CPOP is compatible with CMake, source code and installation guide are accessible through the web page http://cpop.in2p3.fr. In Table 1 are listed the mandatory compilation options concerning Geant4 and CPOP.

Table 1. Lists of mandatory options for compiling Geant4 and CPOP

Geant4 compilation	**CPOP compilation**
GEANT4_USE_SYSTEM_CLHEP	WITH_EXTERNAL_CLHEP
GEANT4_USE_GDML	WITH_GDML_EXPORT
GEANT4_BUILD_MULTITHREADED	WITH_EXAMPLES_BENCHMARK WITH_EXAMPLES_MAS WITH_EXAMPLES_MODELER
GEANT4_USE_OPENGL_X11 GEANT4_USE_QT	WITH_GEANT4_UIVIS WITH_GEANT_4
GEANT4_USE_SYSTEM_EXPAT	WITH_TUTORIALS

2.2.2 The Modeler library

a. Cell conformation and properties

Each cell, part of 2D or 3D cell populations, is considered as a unique entity for which a set of exhaustive characteristics can be settled (nucleus radius, cell membrane radius, forces, cytoplasm and nucleoplasm materials) as well as dynamics (direction, orientation and speed). These features enable to propose in silico cell models adapted to biological outcomes.

Therefore, cell conformation and properties are managed through the 'Models' family classes encompassing 'Environment', 'Organelle', 'Cell Properties', 'Force' and 'RoundCell' classes.

- The 'Environment' class describes cell population geometry, the spatial delimitation for each cell and the spatial delimitation for the whole cell population.

- The ‘Organelle’ class is managing all the biological compartments of a cell. The only organelle currently modelled is the nucleus with a non-deformable spherical shape.
- The ‘Cell Properties’ class is about properties of cells composing the population. User can provide a range of values for the following parameters: nucleus radius, cell membrane radius, nucleus and cytoplasm materials.
- The ‘Force’ class concerns the elastic force applied to cells. Intensity of the elastic force is defined with the ‘rigidity’ parameter to keep low enough in order that convergence is not too fast (usually ‘rigidity’ constant=0.002), and the ‘ratioToStableLength’ parameter of the elastic force defining the level of compaction of the cell population. If this parameter is equal to 1 then, cells are just close to each other, when inferior to 1, then cells are compacted, and when superior to 1, cells are separated as shown in Figure 3.

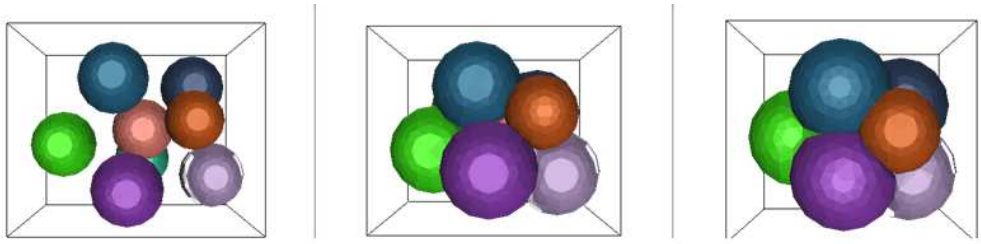

(a) (b) (c)

Figure 3 . Representation of cell population with ratioToStableLength parameter equal to 1.4 (a), 0.85 (b) and 0.7 (c)

- The ‘RoundCell’ class considers each cell as a deformable round cell. In order to adapt its conformation with other cells of the population, each cell is composed of a non-deformable round nucleus positioned at cell barycenter when cell is distorted or at the cell center when cell is perfectly round.
- As the management of individual cell characteristics is not easily feasible when considering large cell populations (more than a million of cells), a system of distribution has been created in order to allocate a set of characteristics to a set of cells. For each cell parameter (nucleus and cell membrane radius, cytoplasm and nucleoplasm materials), range values can be fixed with a corresponding number of

concerned cells. The distribution can be modified to be either random or normal. For that purpose, CPOP is based on the CLHEP HepRandom module.

b. Cell population geometry

A 3D power-weighted Delaunay triangulation, holding cell neighbourhood relations, is used to spatially represent cells with vertices. To enable that, the 'Delaunay' class uses the CGAL library enhancing the Dynamic Object Delaunay package. The Voronoi tessellation, created with the 'VoronoiMesh' class, is used to represent cell shapes using meshes. Each free cell (having no neighbor cell and a ratioToStableLength parameter equal or higher to 1) is considered to have spherical shape with spherical radius; for cells being in conflict with others, cells are constrained like shown in Figure 4. When neighboring cells and their radii are in conflict (ratioToStableLength parameter inferior to 1), then the radius of each cell is minimized in order to not overlap with any other geometry. Therefore, each cell composing a population has its own volume depending of the level of compaction fixed by the user according to the total amount of cells composing the spheroid and the limits fixed for the nucleus and membrane radii.

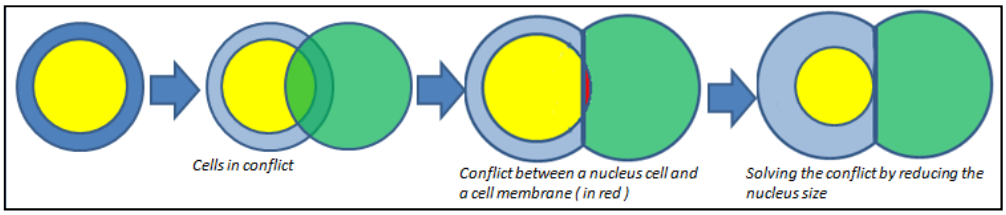

Figure 4. Representation of cells and their radii when cells are compacted

2.2.3 The MAS library

2D and 3D multicellular populations are constructed in order to fit with 2D and 3D biological models (cancer cells) when receiving radiation exposure. To that purpose, the total amount of cells is first distributed homogeneously over a grid system (3D matrix) in order to obtain the final spheroid size of the cell population. Initially, the size of each grid element corresponds to the upper cell membrane radius value. The position of each cell is then easily accessible through this system.

Since cells are distributed along the grid system, each cell is then managed by an agent in charge of applying forces to deal with cell neighbors using a Delaunay triangulation.

The MAS library registers cells at each step till the number of cells requested. Cells are randomly placed on the grid. Other options facilitate the management of cells such as the possibility to fix a displacement threshold or a spatial data structure update after each step execution.

2.3 List of parameters to define a cell population

In Table 2, we listed the parameters to be fixed by the user in order to create a 3D cell population. Those parameters are defined in a configuration file (config.cfg). The 3D cell population is then generated with a visualization interface using the following command line:

```
./generatePopulation -f config.cfg -- vis
```

Table 2 Parameter names, their description to generate a 3D cell population in Figure 5(c).

Parameter name	Description
Cell properties	
nucleusRadius	Radius of the nucleus (µm)
membraneRadius	Radius of the cell (µm)
cytoplasmMaterials	Materials composing the cytoplasm
nucleusMaterials	Materials composing the nucleus
Spheroid properties	
internalRadius	Internal radius of the spheroid (µm)
externalRadius	External radius of the spheroid (µm)
nbCell	Number of cells composing the spheroid
Mesh properties	
maxNumberOfFacetPerCell	Maximum number of facets to represent round cells
Force properties	
ratioToStableLength	Ratio of elastic length
rigidity	Intensity of the force
Simulation properties	
Duration	Duration of the simulation (second)
numberOfAgentToExecute	Number of agents to execute
DisplacementThreshold	Threshold for cell displacement
stepDuration	Duration of a step (second)

The user has the possibility to generate cell populations using or not force and grid system. In Figure 5(a) is presented an example of 3D cell population created using a grid system and no force; in Figure 5(b), the same population created without the grid system.

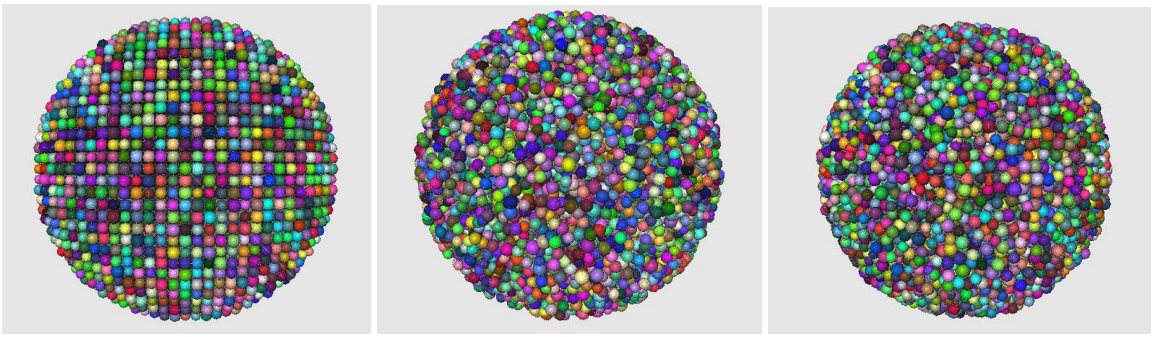

(a) (b) (c)

Figure 5. Spheroid generated using (a) a grid system, (b) without a grid system, (for both simulations, no force is applied), (c) with elastic forces (rigidity=0.002 and ratioToStableLength=0.7)

In Figure 5(c), an example 3D cell population is generated using elastic forces with a rigidity parameter fixed to 0.002 and a ratioToStableLength equal to 0.7. A number of 18124 cells have been generated corresponding to the maximum number of cells that can be contained in a spheroid of 550 µm in diameter with a cell nucleus radius between 4.6 and 6.6 µm and a cell membrane radius between 7.35 and 9.85 µm. The duration of the simulation was 60 seconds and the step duration was fixed to 1 second.

2.4 Specific functionalities for cell irradiation simulations

In order to use 3D cell population models with particle physics simulations in the objective to calculate energy depositions to cells after radiation exposure, the CPOP platform has been designed in order to be compatible with the Geant4 toolkit. Two ways are proposed to use 3D cell population geometry with Geant4 simulations:

- The first way consists in generating cell populations with the CPOP platform in order to create a XML file describing the geometry. Then, the XML file can be interpreted in Geant4 simulations. In this case, it remains the responsibility of the user to implement its own Geant4 application.
- A second way consists in simulating energy depositions using the Geant4 toolkit through CPOP. User has to fix each segment of the track (called step) to a maximum value (called *StepMax)* of about 1/10 to 1/20 of a cell geometry in order to correctly simulate energy depositions. Energy depositions are automatically calculated and allocated to cell population geometry described using a XML file.

In Table 3 are listed the parameters and the associated command lines to be fixed to irradiate a 3D cell population with the Geant4 toolkit embedded in CPOP using a macro file. Energy depositions are recovered in the spheroid defined with three virtual layers (called necrosis, intermediary and external); these layers correspond to what is observed experimentally for cell proliferation with the distribution of diffused oxygen, CO2, and nutrition leading to a proliferating zone (corresponding to external layer), a quiescent viable cell zone (corresponding to intermediary layer) and a necrotic core [39]. Source particles are generated isotropically in the cell population with energies from an energy spectrum provided by the user. Any type of particles can be set as described in Table 3.

CPOP has also been designed to evaluate a potential dose enhancement using nanoparticles when in contact with cell populations during radiation exposure. Nanoparticles are not simulated with their associated geometry but the user has the possibility to set up a combination of energy spectra (that have been pre-generated in the vicinity of a nanoparticle using GATE Monte Carlo simulations for example). The user can specify the number of nanoparticles to simulate, the type of particle to generate isotropically according to an energy spectrum and also can specify the random distribution of nanoparticles in spheroid layers and in the cells (cell membrane, cytoplasm, nucleus membrane and nucleus). When nanoparticles are distributed in membranes, it means that particles are emitted around nucleus or cytoplasm.

All parameters associated to these features are listed in Table 3.

Table 3. Name of classes, parameter names and corresponding command lines for the management of 3D cell population in CPOP with associated radiation exposure.

3D CELL POPULATION UNDER RADIATION	
Parameter name or function	**Command line**
Maximum step size	`/cpop/physics/stepMax value [unit]`
Cuts	`/run/setCut value [unit]`
Geant4 Physics List	`/cpop/physics/physicsList name`
worldSize	`/detector/size value`
Maximum number of facets to describe cells	`/cpop/population/numberFacet value`
Number of sampling cell per layer	`/cpop/population/sampling value`
env	`/cpop/population/input 3DcellPopulation.xml`
Necrosis layer from 0 to value = ratio×spheroid radius	`/cpop/population/internalRatio value`
Intermediary layer from internal ratio to value= ratio×spheroid radius	`/cpop/population/intermediaryRatio value`

Selection of a homogeneous source with a name,
a type of particle,
a spectrum
the total number of particles to emit
	`/cpop/source/addHomogeneous name`
	`/cpop/source/name/particle e-`
	`/cpop/source/name/spectrum spectrum.txt`
	`/cpop/source/name/totalParticle value`

The name of the ROOT output file	`/analysis/setFileName file.root`
3D CELL POPULATION UNDER RADIATION WITH NANOPARTICLES	

Selection of nanoparticles with a name,
a type of particle,
a spectrum,
the number of nanoparticles in the spheroid,
the number of particles to emit per nanoparticle,
the number of nanoparticles to distribute in necrosis/intermediary/external
their distribution in cell membrane, nucleoplasm, nucleus membrane and cytoplasm
	`/cpop/source/addNanoparticle name`
	`/cpop/source/name/particle e-`
	`/cpop/source/name/spectrum spectrum.txt`
	`/cpop/source/name/totalNanoParticle value`
	`/cpop/source/name/particlePerNano value`
	`/cpop/source/name/distributionInRegion value value value`
	
	`/cpop/source/name/distributionInCell value value value value`

2.5 Simulation of SK-MEL28 spheroids under low energy X-ray exposure

In this paper, we decided to reproduce cell irradiations performed with a X-RAD 320 Biological Irradiator (Precision XRay Inc., North Branford, CT), which generates orthovoltage X-rays. The dimensions and positions of various components including the source, the aluminum filter and the collimator within the X-RAD 320 irradiator were simulated using the GATE version 9.0 Monte Carlo platform (with Geant4 version 10.06.p03). In Figure 6 is represented the energy spectrum of X-RAD 320 derived from measurements that has been used as source spectrum in the GATE simulation. The G4EmLivermorePhysics constructor was adopted. Dosimetry (depth dose and dose profiles) obtained after simulation in a water phantom was validated in a previous work [40].

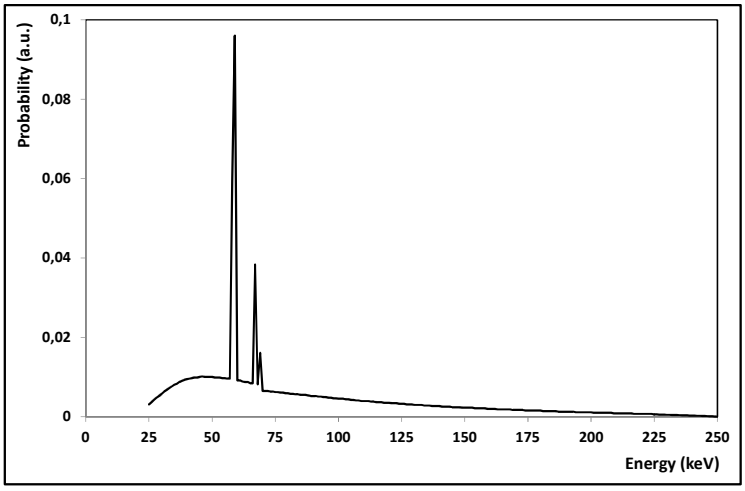

Figure 6. Energy spectrum of X-RAD 320 system derived from measurements.

The range cut was fixed to 1 µm for photons. The energy spectrum of secondary photons to obtain a 1 Gy absorbed dose in a water sphere of 550 µm (corresponding to the spheroid diameter) at 2 cm depth is presented in Figure 7. The photon energy spectrum has been used in CPOP to generate randomly and homogeneously gamma particles in the cell population described in section 3.2. The energy spectrum corresponding to secondary photons (Figure 7) has also been used as source spectrum to irradiate Gadolinium nanoparticles when present in the spheroid.

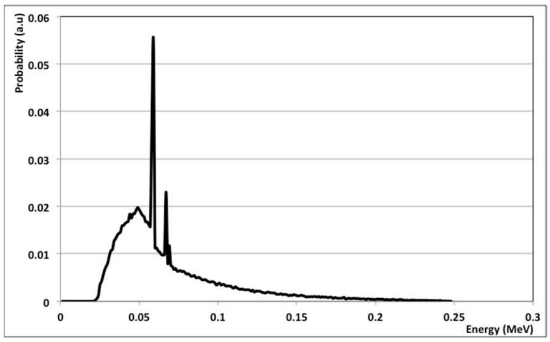

1

Figure 7. Photon energy spectrum entering a water sphere of 550 µm at 2 cm depth.

We recovered energy depositions in the spheroid defined with three virtual layers (called necrosis, intermediary and external). In our use case, the necrosis layer radius is 56.25 µm (corresponding to ¼ of spheroid radius), the intermediary layer is from 56.25 µm to 168.75 µm (corresponding to spheroid radius - ¼ of spheroid radius) and then the external layer is from 168.75 µm to 225 µm. Ten cells are sampled randomly in each layer to collect energy deposited to cytoplasm and nucleus. The Penelope physics list has been set. This choice was done in order to be able to track secondary electrons down to 100 eV and to save computing times with respect to the Geant4 Very Low Energy Extensions (Geant4-DNA) [19]. Atomic deexcitation, including Auger electron emission and fluorescence, were modeled in the simulation. Results are stored in a ROOT file [41] containing an "Edep" tree with the following leaves:

- posX, posY, posZ: the positions in X, Y and Z of the interactions
- edep : the deposited energy

- organelle: the type of organelles considered
- region: the virtual layers (necrosis, intermediary and external)
- cell ID: the ID of sampled cells in the spheroid

2.6 Simulation of SK-MEL28 spheroids under low energy X-ray exposure with GBN

For this paper, simulations are conducted in order to reproduce experiments with AGuIX AC13 nanoparticles, assumed to be spheres of 3.5 nm in diameter and a mass of about 8.5 kDa with the following chemical formula: $Gd_{10}Si_{30}C_{200}N_{50}O_{150}H_{577}$ according to manufacturer's specifications [42]. Therefore, in order to obtain the energy spectrum of secondaries collected at the surface of a GBN, we simulated, with the GATE platform, the GBN as a sphere of 3.5 nm having the same characteristics as cited just before. As spheroids are usually incubated with a GBN concentration of 4 mM (corresponding to a density of 0.034 $g.cm^{-3}$), we fixed a density of 1.034 $g.cm^{-3}$ for the GBN modeled. Penelope physics models have been selected to track secondary electrons down to 100 eV (corresponding to a range limit of 10 nm in liquid water); this limit is higher than the GBN dimension and therefore some very low energy electrons, that could be responsible for cell damage, are not simulated. Atomic deexcitation, including Auger electron emission and fluorescence, were modeled in the simulation. Only the photon energy spectrum in Figure 7 is used (secondary electrons produced in liquid water in the vicinity of the GBN were not considered in this study) as circular source of same diameter as the nanoparticle (3.5 nm), photons are emitted in the direction of the nanoparticle which is located in a vacuum medium, high energy thresholds are fixed in the surrounding volume in order to collect electrons only produced in the nanoparticle and exiting its volume. The energy spectrum of secondary electrons exiting the GBN (GBN_spectrum.spec) is shown in Figure 8.

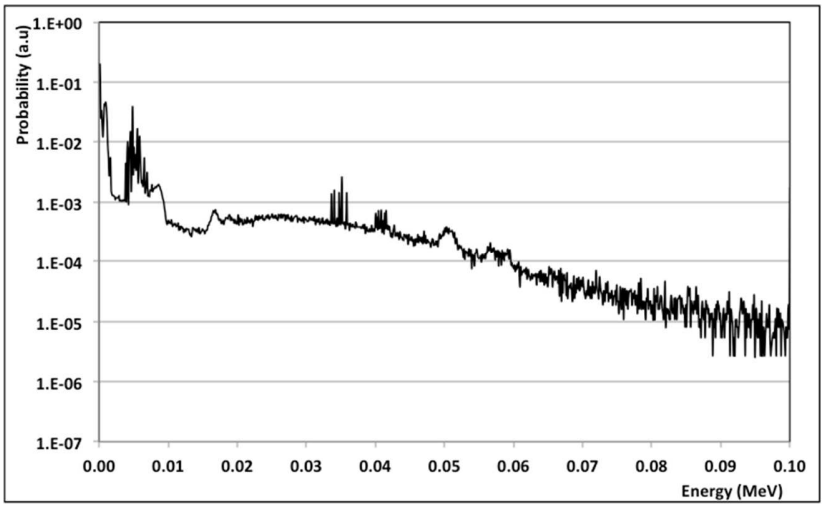

Figure 8. Energy spectrum of secondary electrons (GBN_spectrum.spec) collected at the surface of a AGuIX AC13 GBN.

From Figure 8, we can identify characteristic peaks correlated to atomic relaxation and binding energies of Gadolinium element. Predominant electrons are photoelectrons from the K shell and Auger electrons (emitting from L, M and higher shells). K shell electrons are one order of magnitude more important than Auger electrons.

Many authors [42–45] analyzed the cellular uptake and localization of GBNs in cells by confocal microscopy during a period of observation. AGuIX GBNs have shown exclusively cytoplasmic localization. Further, recent analyses have shown a GBN binding in the external layer of the spheroid. Therefore, we simulated 100% of the GBNs in cell cytoplasm and we used the spectrum obtained in Figure 7 to simulate secondary photons in all layers of the 3D cell population, while we used different proportions of spectra shown in Figure 8 to simulate secondary electrons in the vicinity of GBNs located in cell cytoplasm in the external layer.

3. Results and discussion

For all following applications, we focused only on 3D cell models. It has to be noticed that everything is also applicable for 2D cell populations.

3.1 Generation of 3D cell populations

In Table 4 are listed all the parameters to be fixed in order to create a SK-MEL28 3D cell populations showed in Figure 9.

Table 4. Parameter names and values (or range of values) associated to the description of 3D SkMel28 cell populations described in Figure 9.

Parameter name	Value or range of values		
	Figure 9(a)	Figure 9(b)	Figure 9(c)
nucleusRadius	4.6 – 6.6		
membraneRadius	7.35 – 9.85		
cytoplasmMaterials	G4_WATER		
nucleusMaterials	G4_WATER		
internalRadius	0		
externalRadius	225		
nbCell	962	989	989
maxNumberOfFacetPerCell	300		
ratioToStableLength	0	0.7	0.7
rigidity	0	0.0007	0.002
Duration	60		
numberOfAgentToExecute	100		
DisplacementThreshold	0.5		
stepDuration	1		

In Figure 9, we simulated a realistic cell population (around a thousand of cells) corresponding to SK-MEL 28 melanoma cells observed experimentally through confocal microscopy. Parameters describing this cell population are the same as presented in Table 2. In Figure 9(a) is presented the spheroid obtained without any forces applied, in Figure 9(b) and (c) are presented the spheroids obtained with different force intensities (0.0007 and 0.002 respectively). The spheroid used in the following studies corresponds to the one from Figure 9(a), reaching 962 cells.

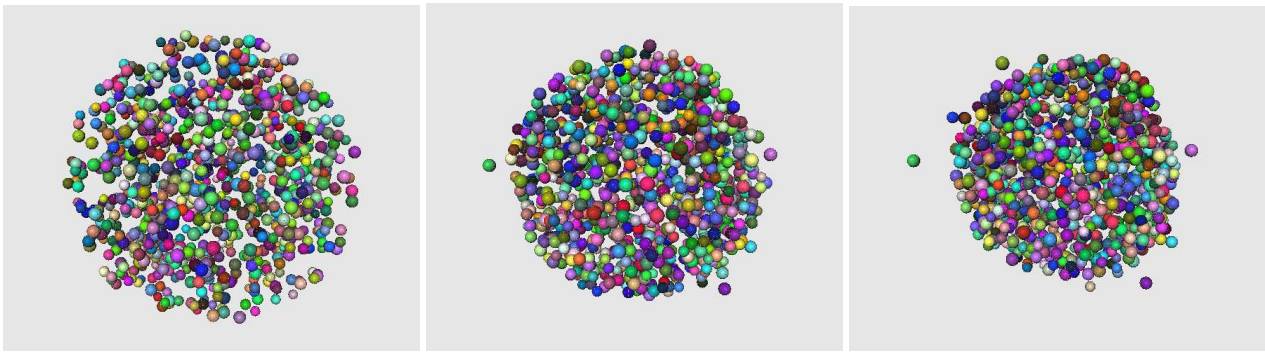

(a) (b) (c)

Figure 9. Spheroids corresponding to SK-MEL28 cell populations. (a) 962 cells generated without forces (defined as 3DCellPopulation.xml in the following studies), (b) 989 cells generated with a force rigidity=0.0007, (c) 989 cells generated with a force rigidity=0.002.

3.2 3D cell population under radiation exposure

We simulated the 3D SK-MEL28 cell population described in Figure 9 (a) under X-ray radiation using the photon spectrum (ph_spectrum.spec) described in Figure 7 and using the GBN spectrum from Figure 8 with nanoparticles. In Table 5 are listed all the parameters used.

In case of radiation exposure without GBN, we obtained the deposited energy in the three virtual layers as shown in Figure 10. The amount of energy deposited in the three layers is comparable. For very low energies, a slight increase on the energy deposited is found in the necrosis layer.

Table 5. Parameter names and corresponding values for the 3D SK-MEL28 cell population under X-ray radiation with and without GBN.

Parameter or function name	**Radiation exposure without GBN**	**Radiation exposure with GBN**	
		Case 1	Case 2
Maximum step size	1 µm	1 µm	
Cuts	100 eV		
Geant4 Physics List	Penelope		
worldSize	800 µm		
Maximum number of facets to describe cells	100		
Number of sampling cell per layer	10		
env	SK-MEL28population.xml		
Necrosis layer radius	56.25 µm		
Intermediary layer radius	56.25 µm to 168.75 µm		
External layer radius	168.75 µm to 225 µm		
Source particles	photons		
Spectrum	ph_spectrum.spec		
Total number of particles emitted	10^7		
Number of nanoparticles in the spheroid	---	10^5	
Type of particles		electrons	
Spectrum		GBN_spectrum.spec	
Number of particles to emit per nanoparticle	---	10	
Number of nanoparticles to distribute in necrosis / intermediary / external	---	$0/0/10^5$	$0/5.10^4/5.10^4$
Distribution in cell membrane / nucleoplasm / nucleus membrane / cytoplasm	---	0/0/0/1	0/0/0/1

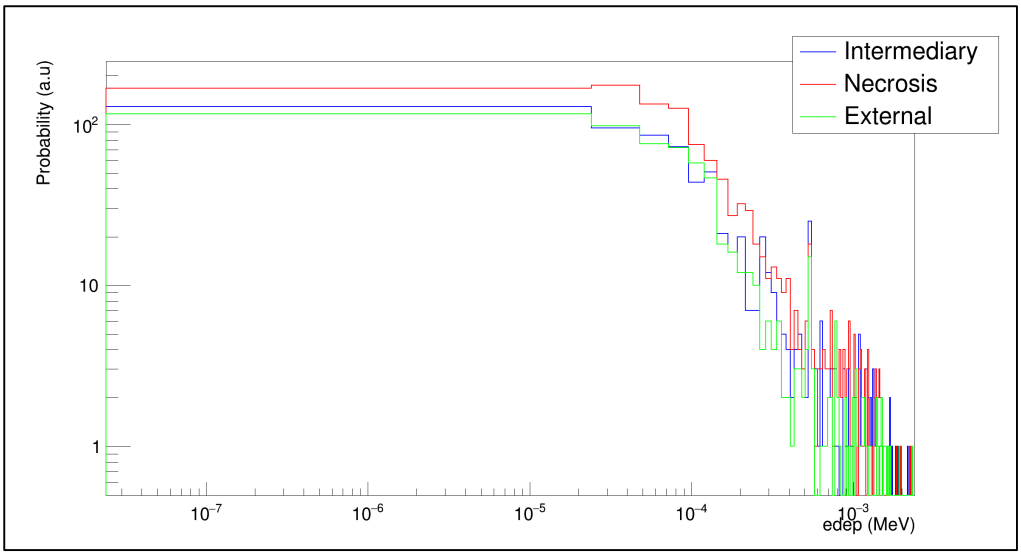

Figure 10. Energy spectra obtained in the spheroid for three virtual layers (External in green, Intermediary in blue and Necrosis in red)

Energy enhancement from GBN in the spheroid

In Figure 11, we show the energy enhancement produced by the presence of 10^5 GBN randomly positioned in the external layer and generating 10 electrons (this value has been selected in order to test the capability of the platform but does not correspond to any experimental observations) with energy selected in the GBN_spectrum.spec. In this configuration, 98% of the energy deposited is due to the presence of GBN. This set-up does not correspond to any experimental outcomes but it shows that we can evaluate the concrete impact on energy deposited in presence of nanoparticles.

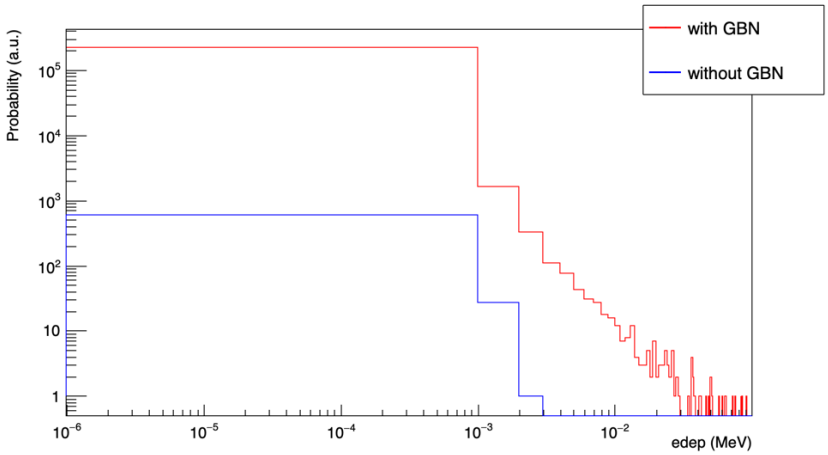

Figure 11. Energy spectra obtained in the external layer of the spheroid with and without GBN.

Influence of the distribution of nanoparticles in the virtual spheroid layers

Then, we set up two simulations (case 1 and 2 in Table 5) with 10^5 GBN located in cell cytoplasm, either totally distributed in the external spheroid layer (case 1) or distributed half in the intermediary and half in the external layer (case 2) as shown in Figure 12. In case 1, energy is mostly delivered in the external and intermediary layer whereas necrosis layer presents a lower contribution. In case 2, we suppose that GBN are penetrating more inside the spheroid till the intermediary region, therefore, energy deposited in the necrosis layer is increased.

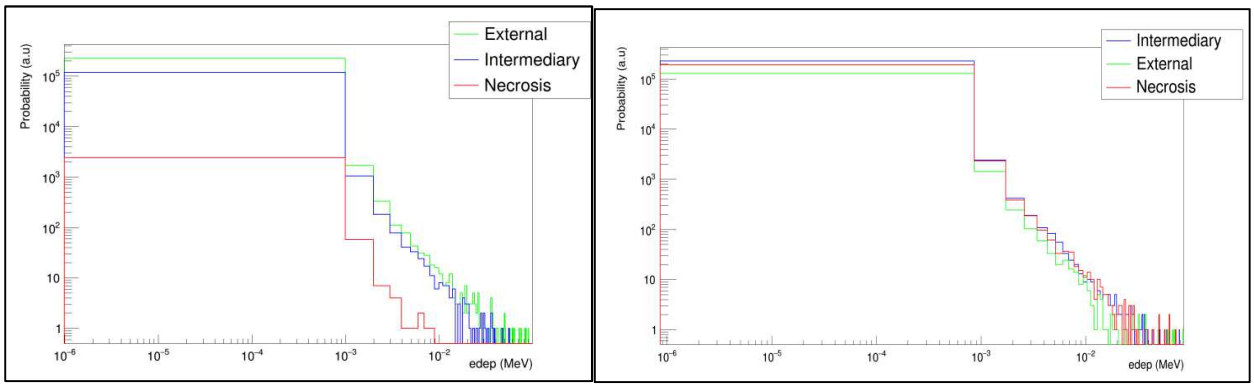

Case 1 Case 2

Figure 12. Energy spectra obtained in the spheroid for three virtual layers (External in green, Intermediary in blue and Necrosis in red)

4. Conclusion

In this paper, we present a new platform which has been combined to the Geant4 toolkit in the objective to simulate three-dimensional cell populations (or spheroids) under radiation. The CPOP platform is able to model deformable cells and their round nuclei submitted to elastic forces in order to reach spheroid geometry corresponding to what can be observed during *in vitro* experiments. Users have the possibility to change and adapt different parameters concerning the cell population (the number of cells, the cell and nucleus mean radii…) and they can also apply different energy spectra to the cell population and cell organelles in order to reproduce what could be observed when cells are in contact with nanoparticles or radiopharmaceutics.

In this study, we demonstrate that the platform is able to reproduce a 3D melanoma cell population composed of a thousand cells. This cell population has been then exposed to specific energy spectra computed with the GATE platform: the energy spectrum of secondary electrons produced in the vicinity of the cell population when irradiated with a X-ray irradiator and secondary electron spectrum produced around a GBN. CPOP, making use of Geant4 with the Penelope physics list, provides mean energy spectra to desired cell organelles in the virtual layers of the spheroid. We showed that an energy enhancement ratio (EER) can be accurately evaluated for different proportions of GBNs in cell organelles.

The platform is freely accessible at cpop.in2p3.fr. Further work includes the usage of the Geant4-DNA physics list with the simulation of complete Auger cascades and the modeling of the production and transport of free radicals from water radiolysis [46].

Acknowledgments

This work is part of the RACE (Radiation resistance of cancer cells using Geant4-DNA) project supported by grants from Plan Cancer 2009-2013 French national initiative through the call for proposals “Domaine de la physique, des mathématiques ou des sciences de l’ingénieur appliqués au Cancer” managed by INSERM (Institut National de la Santé et de la Recherche Médicale) under contract PC201320. This work was also performed within the framework of the LABEX PRIMES (ANR-11-LABEX-0063) of Université de Lyon within the program "Investissements d'Avenir" (ANR-11-IDEX-0007) operated by the French National Research Agency (ANR).

References

[1] Forster JC, Marcu LG, Bezak E. Approaches to combat hypoxia in cancer therapy and the potential for in silico models in their evaluation. Phys Med Eur J Med Phys 2019;64:145–56. https://doi.org/10.1016/J.EJMP.2019.07.006.

[2] Leong DT, Ng KW. Probing the relevance of 3D cancer models in nanomedicine research. Adv Drug Deliv Rev 2014;79–80:95–106. https://doi.org/10.1016/j.addr.2014.06.007.

[3] Taupin F, Flaender M, Delorme R, Brochard T, Mayol J-F, Arnaud J, et al. Gadolinium nanoparticles and contrast agent as radiation sensitizers. Phys Med Biol 2015;60:4449–64. https://doi.org/10.1088/0031-9155/60/11/4449.

[4] Baro J, Sempau J, Fernandez-Varea JM, Salvat F. PENELOPE: an algorithm for Monte Carlo simulation

of the penetration and energy loss of electrons and positrons in matter. Nucl Instruments Methods Phys Res Sect B Beam Interact with Mater Atoms 1995;100:31–46.
[5] Jones BL, Krishnan S, Cho SH. Estimation of microscopic dose enhancement factor around gold nanoparticles by Monte Carlo calculations. Med Phys 2010;37. https://doi.org/10.1118/1.3455703.
[6] Chow JCL, Leung MKK, Jaffray D a. Monte Carlo simulation on a gold nanoparticle irradiated by electron beams. Phys Med Biol 2012;57:3323–31. https://doi.org/10.1088/0031-9155/57/11/3323.
[7] Semenenko V a, Turner JE, Borak TB. NOREC, a Monte Carlo code for simulating electron tracks in liquid water. Radiat Environ Biophys 2003;42:213–7. https://doi.org/10.1007/s00411-003-0201-z.
[8] Li WB, Belchior A, Beuve M, Chen YZ, Di Maria S, Friedland W, et al. Intercomparison of dose enhancement ratio and secondary electron spectra for gold nanoparticles irradiated by X-rays calculated using multiple Monte Carlo simulation codes. Phys Med 2020;69:147–63. https://doi.org/10.1016/j.ejmp.2019.12.011.
[9] Li WB, Beuve M, Di Maria S, Friedland W, Heide B, Klapproth AP, et al. Corrigendum to "Intercomparison of dose enhancement ratio and secondary electron spectra for gold nanoparticles irradiated by X-rays calculated using multiple Monte Carlo simulation codes" [Phys. Med. 69 (2020) 147–163] (Physica Medica (2020) 69 (147–163), (S1120179719305320), (10.1016/j.ejmp.2019.12.011)). Phys Med 2020;80:383–8. https://doi.org/10.1016/j.ejmp.2020.10.008.
[10] Sakata D, Kyriakou I, Tran HN, Bordage MC, Rosenfeld A, Ivanchenko V, et al. Electron track structure simulations in a gold nanoparticle using Geant4-DNA. Phys Med 2019;63:98–104. https://doi.org/10.1016/j.ejmp.2019.05.023.
[11] Poignant F, Monini C, Testa É, Beuve M. Influence of gold nanoparticles embedded in water on nanodosimetry for keV photon irradiation. Med Phys 2021;48:1874–83. https://doi.org/10.1002/mp.14576.
[12] Wälzlein C, Scifoni E, Krämer M, Durante M. Simulations of dose enhancement for heavy atom nanoparticles irradiated by protons. Phys Med Biol 2014;59:1441–58. https://doi.org/10.1088/0031-9155/59/6/1441.
[13] Lin Y, McMahon SJ, Paganetti H, Schuemann J. Biological modeling of gold nanoparticle enhanced radiotherapy for proton therapy. Phys Med Biol 2015;60:4149–68. https://doi.org/10.1088/0031-9155/60/10/4149.
[14] Lin Y, McMahon SJ, Scarpelli M, Paganetti H, Schuemann J. Comparing gold nano-particle enhanced radiotherapy with protons, megavoltage photons and kilovoltage photons: a Monte Carlo simulation. Phys Med Biol 2014;59:7675–89. https://doi.org/10.1088/0031-9155/59/24/7675.
[15] Martínez-Rovira I, Prezado Y. Evaluation of the local dose enhancement in the combination of proton therapy and nanoparticles. Med Phys 2015;42:6703–10. https://doi.org/10.1118/1.4934370.
[16] McKinnon S, Engels E, Tehei M, Konstantinov K, Corde S, Oktaria S, et al. Study of the effect of ceramic Ta2O5 nanoparticle distribution on cellular dose enhancement in a kilovoltage photon field. Phys Med 2016;32:1216–24. https://doi.org/10.1016/j.ejmp.2016.09.006.
[17] McKinnon S, Guatelli S, Incerti S, Ivanchenko V, Konstantinov K, Corde S, et al. Local dose enhancement of proton therapy by ceramic oxide nanoparticles investigated with Geant4 simulations. Phys Med 2016;32:1584–93. https://doi.org/10.1016/j.ejmp.2016.11.112.
[18] Incerti S, Ivanchenko A, Karamitros M, Mantero A, Moretto P, Tran HN, et al. Comparison of GEANT4 very low energy cross section models with experimental data in water. Med Phys 2010;37:4692–708.
[19] Bernal MA, Bordage MC, Brown JMC, Davídková M, Delage E, El Bitar Z, et al. Track structure modeling in liquid water: A review of the Geant4-DNA very low energy extension of the Geant4 Monte Carlo simulation toolkit. Phys Med 2015:1–14. https://doi.org/10.1016/j.ejmp.2015.10.087.
[20] Douglass M, Bezak E, Penfold S. Development of a randomized 3D cell model for Monte Carlo microdosimetry simulations. Med Phys 2012;39:3509. https://doi.org/10.1118/1.4719963.
[21] Kempf H, Bleicher M, Meyer-Hermann M. Spatio-temporal cell dynamics in tumour spheroid irradiation. Eur Phys J D 2010;60:177–93. https://doi.org/10.1140/epjd/e2010-00178-4.
[22] Schaller G, Meyer-Hermann M. Multicellular tumor spheroid in an off-lattice Voronoi-Delaunay cell model. Phys Rev E 2005;71:1–16. https://doi.org/10.1103/PhysRevE.71.051910.
[23] Meyer-Hermann M. Delaunay-Object-Dynamics: Cell Mechanics with a 3D Kinetic and Dynamic

Weighted Delaunay-Triangulation. Curr. Top. Dev. Biol., vol. 81, 2008, p. 373–99. https://doi.org/10.1016/S0070-2153(07)81013-1.
[24] Lee K-N, Jung W-G. Dose response analysis program (DREAP): A user-friendly program for the analyses of radiation-induced biological responses utilizing established deterministic models at cell population and organ scales. Phys Med Eur J Med Phys 2019;64:132–44. https://doi.org/10.1016/J.EJMP.2019.06.013.
[25] DeCunha JM, Poole CM, Vallières M, Torres J, Camilleri-Broët S, Rayes RF, et al. Development of patient-specific 3D models from histopathological samples for applications in radiation therapy. Phys Med Eur J Med Phys 2021;81:162–9. https://doi.org/10.1016/J.EJMP.2020.12.009.
[26] Lee BH, Wang C-KC. A cell-by-cell Monte Carlo simulation for assessing radiation-induced DNA double strand breaks. Phys Med Eur J Med Phys 2019;62:140–51. https://doi.org/10.1016/J.EJMP.2019.05.006.
[27] Barberet P, Vianna F, Karamitros M, Brun T, Gordillo N, Moretto P, et al. Monte-Carlo dosimetry on a realistic cell monolayer geometry exposed to alpha particles. Phys Med Biol 2012;57:2189–207. https://doi.org/10.1088/0031-9155/57/8/2189.
[28] Mirams GR, Arthurs CJ, Bernabeu MO, Bordas R, Cooper J, Corrias A, et al. Chaste: An Open Source C++ Library for Computational Physiology and Biology. PLoS Comput Biol 2013;9:e1002970. https://doi.org/10.1371/journal.pcbi.1002970.
[29] Swat MH, Thomas GL, Belmonte JM, Shirinifard A, Hmeljak D, Glazier JA. Multi-scale modeling of tissues using CompuCell3D. Methods Cell Biol 2012;110:325–66. https://doi.org/10.1016/B978-0-12-388403-9.00013-8.
[30] The CGAL Project. {CGAL} User and Reference Manual. 4.10. CGAL Editorial Board; 2017.
[31] Allison J, Amako K, Apostolakis J, Araujo H, Arce Dubois P, Asai M, et al. Geant4 developments and applications. IEEE Trans Nucl Sci 2006;53:270–8. https://doi.org/10.1109/TNS.2006.869826.
[32] Allison J, Amako K, Apostolakis J, Arce P, Asai M, Aso T, et al. Recent developments in G eant 4. Nucl Instruments Methods Phys Res Sect A Accel Spectrometers, Detect Assoc Equip 2016;835:186–225. https://doi.org/10.1016/j.nima.2016.06.125.
[33] Agostinelli S. Geant4—a simulation toolkit. Nucl Instruments Methods Phys Res Sect A Accel Spectrometers, Detect Assoc Equip 2003;506:250–303. https://doi.org/10.1016/S0168-9002(03)01368-8.
[34] Incerti S, Brown JMC, Guatelli S. Advances in Geant4 applications in medicine. Phys Med Eur J Med Phys 2020;70:224–7. https://doi.org/10.1016/J.EJMP.2020.01.019.
[35] Tran HN, Karamitros M, Ivanchenko VN, Guatelli S, McKinnon S, Murakami K, et al. Geant4 Monte Carlo simulation of absorbed dose and radiolysis yields enhancement from a gold nanoparticle under MeV proton irradiation. Nucl Instruments Methods Phys Res Sect B Beam Interact with Mater Atoms 2016;373:126–39. https://doi.org/10.1016/j.nimb.2016.01.017.
[36] Jan S, Santin G, Strul D, Staelens S, Assié K, Autret D, et al. GATE: a simulation toolkit for PET and SPECT. Phys Med Biol 2004;49:4543–61.
[37] Jan S, Benoit D, Becheva E, Carlier T, Cassol F, Descourt P, et al. GATE V6: a major enhancement of the GATE simulation platform enabling modelling of CT and radiotherapy. Phys Med Biol 2011;56:881–901.
[38] Sarrut D, Bardiès M, Boussion N, Freud N, Jan S, Létang J-M, et al. A review of the use and potential of the GATE Monte Carlo simulation code for radiation therapy and dosimetry applications. Med Phys 2014;41:064301. https://doi.org/10.1118/1.4871617.
[39] Lin R-Z, Chang H-Y, Chang H-Y. Recent advances in three-dimensional multicellular spheroid culture for biomedical research. Biotechnol J 2008;3:1172–84. https://doi.org/10.1002/biot.200700228.
[40] Pham QT, Anne A, Bony M, Delage E, Donnarieix D, Dufaure A, et al. Coupling of Geant4-DNA physics models into the GATE Monte Carlo platform: Evaluation of radiation-induced damage for clinical and preclinical radiation therapy beams. Nucl Instruments Methods Phys Res Sect B Beam Interact with Mater Atoms 2015;353:46–55. https://doi.org/10.1016/j.nimb.2015.04.024.
[41] Brun R, Rademakers F. ROOT — An object oriented data analysis framework. Nucl Instruments Methods Phys Res Sect A Accel Spectrometers, Detect Assoc Equip 1997;389:81–6. https://doi.org/10.1016/S0168-9002(97)00048-X.
[42] Detappe A, Kunjachan S, Rottmann J, Robar J, Tsiamas P, Korideck H, et al. AGuIX nanoparticles as a promising platform for image-guided radiation therapy. Cancer Nanotechnol 2015;6:4.

https://doi.org/10.1186/s12645-015-0012-3.
[43] Kotb S, Detappe A, Lux F, Appaix F, Barbier EL, Tran V-L, et al. Gadolinium-Based Nanoparticles and Radiation Therapy for Multiple Brain Melanoma Metastases: Proof of Concept before Phase I Trial. Theranostics 2016;6:418–27. https://doi.org/10.7150/thno.14018.
[44] Adjei IM, Sharma B, Labhasetwar V. Nanoparticles: Cellular Uptake and Cytotoxicity. Adv. Exp. Med. Biol., vol. 811, 2014, p. 73–91. https://doi.org/10.1007/978-94-017-8739-0_5.
[45] Luchette M, Korideck H, Makrigiorgos M, Tillement O, Berbeco R. Radiation dose enhancement of gadolinium-based AGuIX nanoparticles on HeLa cells. Nanomedicine 2014;10. https://doi.org/10.1016/j.nano.2014.06.004.
[46] Karamitros M, Luan S, Bernal MA, Allison J, Baldacchino G, Davidkova M, et al. Diffusion-controlled reactions modeling in Geant4-DNA. J Comput Phys 2014;274:841–82. https://doi.org/10.1016/j.jcp.2014.06.011.